JOURNAL OF CATALYSIS 32, 63–71 (1974)

Interaction Between the Active Components and Support in Co–Mo–Al_2O_3 Systems

P. RATNASAMY, R. P. MEHROTRA, AND A. V. RAMASWAMY

Indian Institute of Petroleum, Dehradun (U.P.), India

Received May 16, 1973

Structural changes in an alumina support in presence of molybdenum and cobalt oxides have been investigated using DTA, TG and X-Ray techniques. The kinetics of crystal growth and sintering in alumina are affected by these two oxides in different ways. Molybdenum oxide accelerates the phase transformations. When cobalt is also present, even though the phase transformations still do occur, the activation energy required is higher. In addition, the products are less crystalline and have smaller crystallite sizes. The relevance of these results to the role of cobalt in Co–Mo–Al_2O_3 hydrodesulfurization catalysts is also discussed.

INTRODUCTION

The structural and textural features of molybdenum sulfide catalytic systems have recently been studied in detail (*1–4*). A similar study of molybdenum sulfide supported on alumina is of interest since this catalyst either alone or with cobalt is widely used for various reactions (*5*). Even though the adsorptive and catalytic activity of these catalysts is well documented, very little is known about their structure and still much less is understood about the correlation between their structure and catalytic activity (*6*). For example, what is the stoichiometry and crystalline structure (if any) of molybdenum sulfide when it is supported on alumina? Does the alumina support undergo any changes when molybdenum oxide is deposited on it and then further reduced to the sulfide? What is the role of cobalt? In the present investigation, the structural changes in an alumina support when molybdenum oxide alone or along with cobalt oxide is deposited on it have been studied using DTA, TG, and X-Ray diffraction techniques.

EXPERIMENTAL METHODS

Materials

Sample A was an amorphous alumina containing γ and η forms. It was obtained from aluminum nitrate and calcined at 550°C. Sample B was obtained by heating sample A in air at 900°C for 2 hr. Samples C and D were obtained by depositing ammonium paramolybdate (13% by wt of MoO_3) on sample A, drying at 110°C and heating in air for 2 hr, at 700 and 900°C, respectively. Samples E and F were from a commercial Co–Mo–Al_2O_3 hydrodesulfurization catalyst calcined in air for 2 hr at 700 and 900°C, respectively. Sample G was prepared by depositing $Co(NO_3)_2$ on sample A (3% by wt of CoO), drying at 110°C and calcining in air for 2 hr at 900°C.

Apparatus

The X-ray patterns were obtained with a G.E.C. (model X RD-6) diffractometer. Copper $K\alpha (\lambda = 1.5418\ \text{Å})$ radiation with nickel filters, scintillation counter and pulse height selector was used. For the DTA measurements (range 100–1000°C) a Linseis instrument was used. α-Al_2O_3 was taken as the standard. The TGA experiments were carried out using a Fischer model (1 mg/mV full scale recorder deflection). A linear heating rate of 5°C/min was maintained for both DTA and TGA experiments which were carried out in air. The reported temperatures are accurate to about ±10°C.

RESULTS

Differential Thermal and Thermogravimetric Analyses

Figure 1 illustrates the thermal effects observed on heating different samples. When the commercial Co–Mo–Al_2O_3 catalyst (Co/Mo = 0.2; activated at 550°C in air) is heated (curve A), the endothermic effect around 100°C is due to the elimination of adsorbed water. Since the catalyst had already been calcined at 550°C, there is no likelihood of constitutional water being present. The exothermic peak at 850°C is interesting since we have observed a similar peak in many commercial Co–Mo–Al_2O_3 hydrodesulfurization catalysts that we have studied (7). Curve B represents the thermal behavior of sample A. The large endothermic peak around 100°C is due to the elimination of adsorbed water. We assign the small peaks at 250 and 500°C to the elimination of

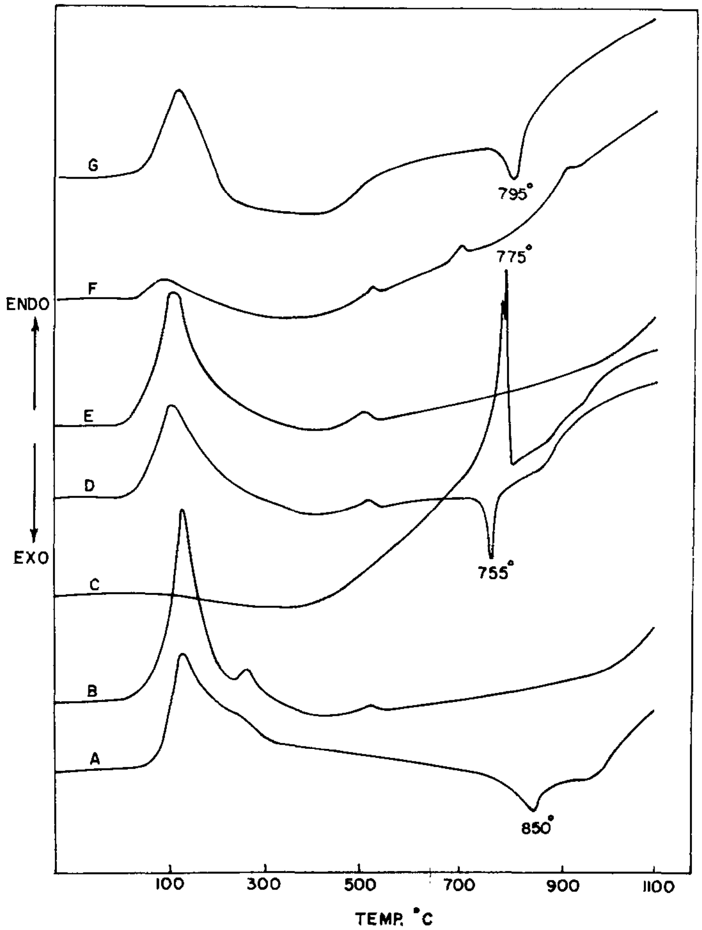

FIG. 1. DTA curves: (A) commercial Co–Mo–Al_2O_3 catalyst; (B) sample A; (C) MoO_3; (D) Mo–sample A; (E) Co–sample A; (F) Mo–α-Al_2O_3; (G) Co–Mo–sample A.

hydroxyl groups from the alumina support. It should be noted that no exothermic peak is observed in the region 700–900°C indicating that, under the conditions of DTA experiment, the alumina sample A does not undergo any perceptible phase modifications. When MoO_3 (obtained from calcining ammonium paramolybdate in air at 500°C for 24 hr) is heated in air, no peaks are seen in the DTA chart (curve C) until a temperature of 780°C is reached when a sharp endothermic peak due to the melting of MoO_3 is observed [mp 795°C (*8*)]. When the product obtained by depositing ammonium paramolybdate on sample A, drying at 110°C and calcining at 550°C is studied by DTA, a sharp exothermic peak is observed at 755°C (curve D). It is interesting that this exothermic phenomenon occurs in the same temperature region where MoO_3 begins to melt (curve C). The significance of this feature is discussed below. It should be emphasized, however, that in the absence of deposited molybdenum oxide, the support alumina alone does not exhibit any exothermic effects, in this temperature region (curve B). To confirm the specificity of molybdenum oxide, cobalt oxide was deposited (from cobalt nitrate) on sample A, (3% by wt of CoO), dried and activated at 550°C under conditions identical to those of the Mo–Al_2O_3 sample. The results are shown in curve E. Apart from the large endothermic peak at 100°C and a small one at 500°C, no exothermic peaks are seen in the region 700–900°C. That the exothermic peak (in curve D) is due to a transformation in the alumina support and not in the supported molyb-

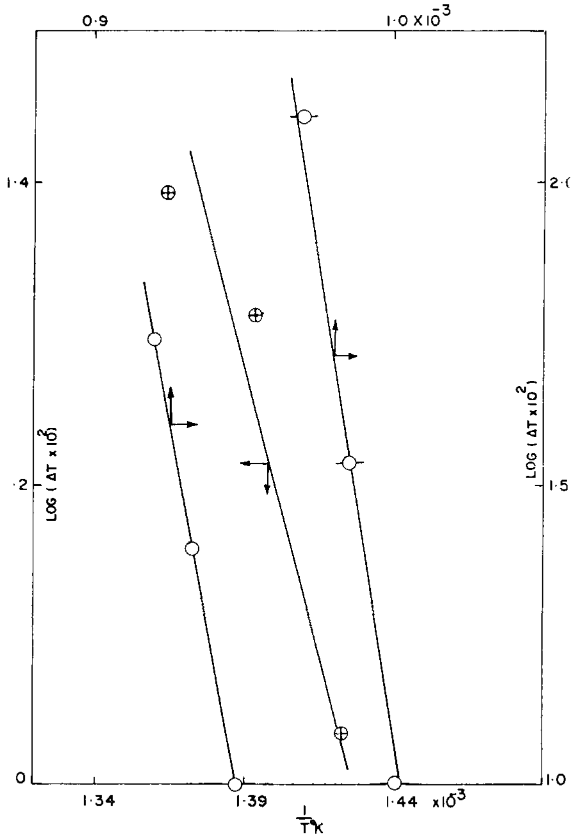

FIG. 2. Arrhenius plots: (⊕) Mo–sample A; (—○—) Co–Mo–sample A; (○) commercial Co–Mo–Al_2O_3 catalyst.

denum oxide phase is seen from curve F. In this case, ammonium paramolybdate was deposited on a sample of α-alumina (confirmed by X-rays), dried at 100°C and calcined in air at 550°C. All conditions were chosen to approximate as nearly as possible those for curve D; only the support was different. The resulting thermogram (curve F) does not show any exothermic peak.

To check whether the exothermic phenomenon was reversible, one of the samples (curve A) was subjected to an up-down-up DTA cycle. The exothermic effect was irreversible in that no peaks were observed during the cooling or reheating cycle. Separate thermogravimetric measurements showed that for both curves A and D there was no weight loss in the temperature range where the exothermic peak is observed. That is, the exothermic effect is due either to a phase transformation and/or crystallite growth in the alumina support and not due to a decomposition of the deposited components.

To probe deeper into the role of cobalt, a Co–Mo–Al_2O_3 catalyst was prepared (Co/Mo = 0.2) by depositing aqueous solutions of cobalt nitrate and ammonium paramolybdate on sample A, drying at 110°C and activating at 550°C. Its thermogram is shown in curve G. Apart from the endothermic peaks at 106 and 496°C, there is a fairly sharp exothermic peak at 795°C. The activation energies for the exothermic transformations (curves A, D and G) were calculated from the experimental DTA curve using the method of Piloyan, Ryabchikov and Novikova (*9*). The Arrhenius plots are shown in Fig. 2. The values of activation energy (from the graph) are 132.8 (curve A, commercial Co–Mo–Al_2O_3), 39.4 (curve D, Mo on sample A) and 141.9 (curve G, Co–Mo on sample A) kcal/mol, respectively. These values have errors of the order of ±15% (*10*). Values of activation energy in the range 120–150 kcal/mol have been obtained also in the case of other commercial catalysts containing both cobalt and molybdenum (*7*). Of course, we are aware of the fact that the activation energy is a questionable concept when applied to solid state transformations (*11*). However, the large difference in the activation energy between samples containing molybdenum alone (about 40 kcal/mol) and those containing molybdenum and cobalt (120–150 kcal/mol) leads to the qualitative conclusion that in the presence of cobalt the solid state transformation of alumina is retarded and requires a much higher activation energy. This retardation by cobalt is also supported by X-ray diffraction results presented below.

X-Ray Diffraction

The aim of the X-ray diffraction experiments was to identify the products of the exothermic solid state transformations. Samples B, C, D, E, F and G were prepared, as detailed earlier, with this point in view. The samples were heated at 700 or 900°C for 2 hr, so that enough product could be formed for identification by X-rays. Conditions of heat treatment were identical for samples C and E, on the one hand, and for samples B, D, F and G on the other. The diffractograms are shown in Fig. 3. The *d* values of the lines as well as the relative intensity ratios and crystallite sizes are given in Table 1. Peak areas were used in computing the I/I_0 values. The crystallite sizes were calculated from the profile width at one half its maximum height, using the Scherrer equation. A value of 1.0 was used for the Scherrer constant, *K*. The profile width due to instrumental broadening was corrected by using a sample of α-alumina of crystallite size greater than 3000 Å. Though the Scherrer equation was derived for a sample of cubic crystals, it is not a bad approximation for other shapes, if, for each *hkl* reflection, the value of *D*, the crystallite size, is interpreted as an average crystal dimension perpendicular to the corresponding reflecting planes (*12*). The main structural features are summarized in the last column of Table 1.

Sample A is a mixture of γ- and η-alumina characterized by broad peaks at 1.953 and 1.401 Å due to *hkl* reflections 400 and 440, respectively, of the spinel (*13*). It

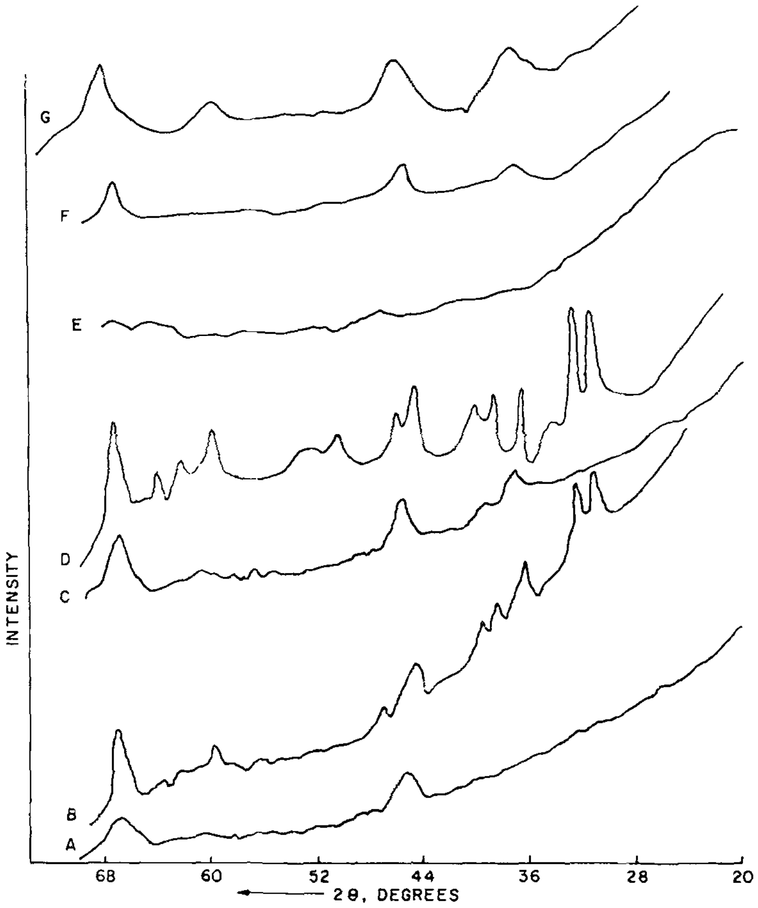

FIG. 3. X-Ray diffractograms. The curves A–G correspond to samples A–G mentioned in the text.

is not possible to estimate the relative proportions of γ and η due to the diffuse nature of the peaks. On heating at 900°C for 2 hr in air (sample B), peaks due to δ- and θ-alumina were observed. Again, it is difficult to obtain their relative proportions. Lippens (*13*) had also arrived at a similar conclusion, namely, that differentiation between γ and η or δ and θ forms of alumina is very difficult and is possible only for well crystalline samples. As expected, the crystallite size increases from sample A to B (35 ± 20 and 42 ± 25 Å to 103 ± 14, 128 ± 20, 148 ± 19, 106 ± 20 and 105 ± 16 Å, respectively). Sample C (containing molybdenum and heated to 700°C) exhibits lines due to γ- and η-alumina. The observed *d* values (2.429, 2.283, 1.989 and 1.406 Å) correspond well with those observed by Lippens (*13*) for a mixture of γ- and η-aluminas (2.397, 2.395; 2.284, 2.284; 1.990, 1.980; and 1.407, 1.396 Å, respectively). Comparison of the relative intensity ratios (Table 1) with those of Lippens further confirms the above assignment. On heating to 900°C (sample D), new lines due to δ and θ forms appear. The observed *d* values (Å) together with those observed by Lippens (in parentheses) for δ- and θ-alumina are: 2.849 (2.859, 2.881), 2.730 (2.731, 2.728), 2.637 (2.557, 2.601), 2.462 (2.462, 2.460), 2.321 (2.314, 2.315), 2.254 (2.264, 2.279), 2.014 (2.028, 1.986), 1.965 (1.913, 1.953), 1.807 (1.800, 1.827), 1.544 (1.538, 1.538), 1.492 (1.484, 1.517), 1.457 (1.456, 1.456) and 1.397 (1.392, 1.396) Å, respectively. The agree-

TABLE 1
X-Ray Diffraction Results

Sample (°C)	d values (Å)	I/I_0	Crystallite size, D(Å)	Structural features of the alumina support
A(500)	1.953[a]	0.880[b]	35 ± 20	Highly amorphous; the crystalline fraction containing a mixture of η- and γ-Al_2O_3
	1.401	1.0	42 ± 25	
B(900)	2.867	0.769	103 ± 14	The crystalline fraction contains predominantly a mixture of δ- and θ-Al_2O_3; some ($\eta + \gamma$) is also present.
	2.763	0.846	128 ± 20	
	2.468	0.538	148 ± 19	
	2.338			
	2.276			
	2.036	0.487	106 ± 20	
	1.933			
	1.551			
	1.397	1.0	105 ± 16	
C(700)	2.429	0.484	104 ± 21	Highly amorphous; η and γ forms are present.
	2.283	0.150		
	1.989	0.774	106 ± 25	
	1.406	1.0	97 ± 14	
D(900)	2.849	0.840	147 ± 20	Mixture of δ- and θ-Al_2O_3; appreciable amount of amorphous phase still present.
	2.730	1.0	177 ± 23	
	2.637			
	2.462	0.720	227 ± 30	
	2.321			
	2.254			
	2.014	0.580	131 ± 21	
	1.965			
	1.807			
	1.544			
	1.492			
	1.457			
	1.397	0.92	114 ± 17	
E(700)	No peaks could be clearly distinguished.			Completely amorphous.
F(900)	2.455	0.500	89 ± 20	The crystalline fraction consists of a mixture of δ and θ forms.
	1.998	0.889	117 ± 18	
	1.401	1.0	126 ± 20	
G(900)	2.840	0.086		The crystalline fraction consists predominantly of η and γ forms; small amount of θ form is also present.
	2.398	0.686		
	1.993	0.999	130 ± 18	
	1.530	0.229		
	1.406	1.0	110 ± 16	

[a] The values are accurate to ±0.003 Å.

[b] Relative intensity values.

ment is satisfactory. Compared to sample B (which was also heated at 900°C for 2 hr) sample D has a larger average crystallite size (147 ± 20, 177 ± 23 and 227 ± 30 against 103 ± 14, 128 ± 20 and 148 ± 19 Å, respectively). In addition, the crystalline fraction is also higher. The total integrated area of the peaks at d = 2.85–2.86, 2.73–2.76 and 2.46 is equal to 12.8 (arbitrary units) in the case of sample D but only 8.4 in the case of sample B. Thus, the presence of molybdenum oxide causes higher crystallinity and larger crystallite sizes for the ($\delta + \theta$) alumina phases. This is evidently a kinetic effect since δ- and θ-aluminas are formed even in the absence of molybdenum oxide when sample A is heated for 2 hr at 900°C (curve B, Fig. 3).

The influence of cobalt (when present along with molybdenum) is shown in Fig. 3, curves E (700°C) and F (900°C), for samples E and F, respectively. At 700°C (curve E, Fig. 3) no peaks are clearly distinguishable. At 900°C (curve F, Fig. 3) the broad peaks at d values of 2.455, 1.998 and 1.401 Å have been assigned to a mixture of δ- and θ-aluminas. The samples containing cobalt plus molybdenum are much less crystalline and their crystallite sizes are smaller than those containing molybdenum alone (Table 1). Since the crystallinity and crystallite size refer only to the alumina support, it may be concluded that the crystallization of the δ- and θ-alumina phases is retarded in the presence of cobalt.

To check whether this effect of cobalt is operative even in the absence of molybdenum, sample G containing cobalt was calcined at 900°C for 2 hr, under conditions identical to those of samples B, D and F. The diffractogram (curve G) reveals the presence of predominantly γ and η forms and only small amounts of δ and θ forms. The relative intensity of the peak at $d = 2.840$ Å characteristic of θ-alumina (*13*), is only 0.0857 for sample G compared to 0.769 and 0.84 for samples B and D, respectively.

DISCUSSION

The salient features of all our results may be summarized as follows: Sample A consists of a mixture of γ- and η-aluminas (Fig. 3, curve A). On sufficiently prolonged heating at 900°C, it transforms into δ- and θ-aluminas (curve B, Fig. 3; Table 1). The kinetics of this transformation is affected by deposited molybdenum and cobalt oxides in different ways. Under the conditions of the DTA experiment, deposited molybdenum oxide brings about this change at 755 ± 10°C (curve D, Fig. 1). Under identical conditions, sample A, either alone or containing deposited cobalt oxide does not undergo any phase transformations (Fig. 1, curves B and E, respectively). When both cobalt and molybdenum are present, even though the phase transformations still do occur, the activation energy is increased (Fig. 2). Moreover, the crystallinity of the products (δ- and θ-aluminas) is lower (curves E and F vs curves C and D, respectively, in Fig. 3). The crystallites are also smaller in size (Table 1). Thus, the presence of cobalt retards the crystallization of the δ and θ phases of alumina, which process would, otherwise have been accelerated with a lower activation energy in the presence of molybdenum oxide. This effect of cobalt is operative even in the absence of molybdenum. Nahim and Huffman (*18*) using electron microscopy had also observed similar effects of molybdena on the phase transformations of γ-alumina.

The Tammann temperature, for alumina, above which bulk diffusion is appreciable is about 880°C [mp 2050°C (*14*)]. Since δ- and θ-aluminas are formed in this region (for samples B and D), there will be a high degree of bulk mobility in the system leading to well crystalline products. This accounts for the sharp peaks in curves B and D of Fig. 3. The rate of surface diffusion, on the other hand, will become appreciable at a such lower temperature, namely about 500°C [0.33 T_{mp}°K (*15*)]. For MoO_3 this temperature is about 100°C. Since all the three exothermic crystallizations (curves A, D and G of Fig. 1) occur between 750 and 850°C, surface diffusion of reaction components will occur on the surface of the alumina particles at these temperatures. MoO_3, present on the surface of alumina (*6*) will be in a molten state at these temperatures and will form a liquid layer around the particles. This will lower the surface energy of the alumina particles and facilitate their sintering (by surface viscous flow, for example) and phase transformation.

Cobalt may react with the alumina or molybdenum oxide. In both the cases, formation of δ- and θ-alumina phases will be retarded, as observed. From magnetic susceptibility studies, Richardson (*16*) had come to the conclusion that below an initial Co/Mo ratio of 0.3 the fresh catalysts (unreduced, nonsulfided, as in our case) contain no $CoAl_2O_4$ and less than 10% of cobalt as CoO, the remainder forming an "active complex" with molybdenum. The absence of $CoAl_2O_4$ and CoO has also been confirmed by Ashley and Mitchell (*6*). Since both the commercial as well as our Co–Mo–Al_2O_3 catalysts have a Co/Mo ratio of 0.2, the possibility of crystalline $CoAl_2O_4$ formation in our samples is unlikely.

There is no X-ray evidence in our studies also, for the presence of crystalline $CoAl_2O_4$. However, since cobalt does retard the crystallization of alumina even in the absence of molybdenum, an interaction between cobalt and the support is established. The nature of this interaction is not clear. It may be of interest to mention here that all the Co–Al_2O_3 samples calcined above 500°C were blue in color, revealing the presence of Co^{2+} ions in a tetrahedral surrounding of O^{2-} ions (*6*b). It is possible that "spinel-like regions" exist in these samples where the short-range order (say, of about 6–10 Å) around Co^{2+} is similar to that in $CoAl_2O_4$, the regions being dimensionally too small to be 'seen' by X-ray diffraction. The presence of such regions in the support structure will, however, stabilize the support against phase transformation to δ and θ forms. The presence of similar regions in other amorphous catalyst systems is well known (*17*).

Formation of $CoMoO_4$ or "active Co–Mo complex" will suppress the formation of a liquid layer around the particles in the temperature region 750–850°C. In the absence of this layer, viscous flow sintering and crystal growth will be more difficult. The phase transformations under these conditions will occur by a different mechanism and hence require a different activation energy as indeed observed experimentally.

Kolboe and Amberg (*19*) had found that the specific thiophene desulfurization activity (per unit area) of many MoS_2, Co–Mo–Al_2O_3 and Cr_2O_3 catalysts was of the same order of magnitude. The differences in their bulk catalytic activity (per g) were due to difference in their surface areas. One of the probable roles of cobalt is to prevent the crystal and/or crystallite growth in the support alumina (with consequent reduction in surface area) which process would otherwise be facilitated by molybdenum oxide, especially during the calcination of the oxide prior to sulfidation.

ACKNOWLEDGMENT

The authors thank Mr. G. Balamalliah for useful discussions and Drs. M. G. Krishna and K. K. Bhattacharyya for encouragement and support.

REFERENCES

1. RATNASAMY, P., AND FRIPIAT, J. J., *Trans. Faraday Soc.* **66**, 2897 (1970).

2. RATNASAMY, P., AND LEONARD, A. J., *J. Catal.* **26**, 352 (1972).

3. RATNASAMY, P., RODRIGUE, L., AND LEONARD, A. J., *J. Phys. Chem.* **77**, 2242 (1973).

4. RATNASAMY, P., unpublished data.

5. SCHUMAN, S. C., AND SHALIK, H., *Catal. Rev.* **4**, 245 (1970).

6. (a) MITCHELL, P. C. H., "The Chemistry of some hydrodesulphurization catalysts containing molybdenum." Climax Molybdenum Co., Ltd., New York, 1967; (b) ASHLEY, J. H., AND MITCHELL, P. C. H., *J. Chem. Soc. Ser. A*, 2821 (1968).

7. RATNASAMY, P., MEHROTRA, R. P., AND RAMASWAMY, A. V., unpublished data.

8. ROSSINI, F. D., WAGMAN, D. D., EVANS, W. H., LEVINE, S., AND JAFFE, I. *Nat. Bur. Stand.* (*U. S.*) *Circ.* **500**, 382 (1952).

9. PILOYAN, F. O., RYABCHIKOV, I. D., AND NOVIKOVA, O. S., *Nature* (*London*) **5067**, 1229 (1966).

10. GARN, P. D., CRC Critical Reviews in *Anal. Chem.* **65** (1972).

11. BERGGREN, G., AND BROWN, A., *in* "Thermal Analysis" (R. F. Schwenker and P. D. Garn, Eds.), p. 881. Academic Press, New York, 1969.

12. WARREN, B. E., "X-Ray Diffraction," p. 251. Addison-Wesley, Reading, MA, 1969.

13. LIPPENS, B. C., Thesis, Delft Univ., 1961.

14. "International Critical Tables." Numerical data 1928, Vol. 1.
15. WELEH, A. J. E., *in* "Chemistry of the Solid State" (W. E. Garner, Ed.), Butterworths, London, 1955.
16. RICHARDSON, J. T., *Ind. Eng. Chem. Fundam.* 3, 154 (1964).
17. RATNASAMY, P., AND LEONARD, A. J., *Catal. Rev.* **6**, 293 (1972).
18. NAHIN, P. G., AND HUFFMAN, H. C., *Ind. Eng. Chem.* **41**, 2021 (1949).
19. KOLBOE, S., AND AMBERG, C. H., *Can. J. Chem.* **44**, 2623 (1966).